

# Toroidal Quadrupole Form Factor of the Deuteron

E. Mereghetti<sup>1</sup>, J. de Vries<sup>2,3,4</sup>, R. G. E. Timmermans<sup>4</sup>, and U. van Kolck<sup>5,6</sup>

<sup>1</sup> *Ernest Orlando Lawrence Berkeley National Laboratory, University of California,  
Berkeley, CA 94720, USA*

<sup>2</sup> *Institute for Advanced Simulation, Institut für Kernphysik, and  
Jülich Center for Hadron Physics, Forschungszentrum Jülich,  
D-52428 Jülich, Germany*

<sup>3</sup> *Nikhef, Science Park 105,  
1098 XG Amsterdam, The Netherlands*

<sup>4</sup> *KVI, University of Groningen,  
9747 AA Groningen, The Netherlands*

<sup>5</sup> *Institut de Physique Nucléaire, Université Paris Sud, CNRS/IN2P3,  
91406 Orsay, France*

<sup>6</sup> *Department of Physics, University of Arizona,  
Tucson, AZ 85721, USA*

## Abstract

We calculate the toroidal quadrupole moment and form factor of the deuteron, which violate time-reversal symmetry but conserve parity, at leading order in two-flavor chiral effective field theory with perturbative pion exchange. We take into account time-reversal and parity violation due to the QCD vacuum angle combined with parity violation resulting from the weak interaction in the Standard Model. We also consider time-reversal and parity violation that at the quark-gluon level results from effective dimension-six operators originating from physics beyond the Standard Model.

# 1 Introduction

It has long been known that particles with non-zero spin can have “toroidal” electromagnetic form factors that are odd under charge conjugation  $C$ , which implies that they violate either parity ( $P$ ) or time reversal ( $T$ ), but not both symmetries simultaneously [1]. The toroidal dipole form factor (TDFF), also called the anapole [2], requires spin 1/2 or higher, violates  $P$  and conserves  $T$ . The toroidal quadrupole form factor (TQFF), which requires spin 1 or higher, violates  $T$  and conserves  $P$ , and so on [3]. Toroidal form factors produce no physical effects when the photon is on-shell, and correspond in a classical picture to fields within the charge distribution [4]. These features contrast with the more familiar  $C$ -even electric and magnetic form factors, which respect or violate both  $P$  and  $T$  simultaneously, and produce effects for on-shell photons. The only form factors allowed for massive particles that are their own antiparticles are toroidal [5].

The toroidal form factors do contribute to the short-range interaction with a charged particle. For nucleons and nuclei, in particular, they are in principle accessible via lepton scattering. While there exist calculations of the TDFFs of the nucleon and nuclei, there is apparently no calculation of a nuclear TQFF. The TQFF of positronium was calculated in Ref. [6].

The aim of this paper is to provide the first controlled calculation of the TQFF of the simplest nucleus, the deuteron, at low momentum. The Lorentz-covariant electromagnetic current of a particle with spin 1 is described by seven electromagnetic form factors: charge, magnetic dipole, and electric quadrupole, which are  $P$ - and  $T$ -conserving ( $PT$ ); electric dipole and magnetic quadrupole, which are  $P$ - and  $T$ -violating ( $P\mathcal{T}$ ); TDFF, which is  $P$ -violating and  $T$ -conserving ( $P\mathcal{T}$ ); and, finally, TQFF, which is  $P$ -conserving and  $T$ -violating ( $P\mathcal{T}$ ). We can write the spatial,  $P\mathcal{T}$  component of the electromagnetic current as [3]

$$\langle \vec{p}', j | J_{PT}^k | \vec{p}, i \rangle = i \left[ q^i q^j q^k - \frac{\vec{q}^2}{2} (\delta^{ik} q^j + \delta^{jk} q^i) \right] F_{PT}(\vec{q}^2), \quad (1)$$

where  $|\vec{p}, i\rangle$  is a deuteron state with momentum  $\vec{p}$  and polarization  $\delta_i^\mu$  in the rest frame, normalized so that  $\langle \vec{p}', j | \vec{p}, i \rangle = \sqrt{1 + \vec{p}^2/m_d^2} (2\pi)^3 \delta^{(3)}(\vec{q}) \delta_{ij}$ ,  $\vec{q} = \vec{p} - \vec{p}'$  is the (outgoing) momentum of the photon,  $m_d = 2m_N - \gamma^2/m_N + \dots$  is the deuteron mass in terms of the nucleon mass  $m_N \simeq 940$  MeV and the binding momentum  $\gamma \simeq 45$  MeV.  $F_{PT}(\vec{q}^2)$  is the TQFF, which is proportional to the proton charge  $e = \sqrt{4\pi\alpha_{\text{em}}}$  and has dimensions of  $\text{mass}^{-3}$ . We express it in units of  $e \text{ fm}^3$ .

We denote the corresponding toroidal quadrupole moment (TQM) by  $\mathcal{T}_d = F_{PT}(0)$ . It can be viewed as an interaction of the deuteron  $d$  with the second derivative of the magnetic field  $\vec{B}$  of the form

$$\mathcal{L} = \frac{\mathcal{T}_d}{2} d^\dagger \{S_i, S_j\} d \nabla_i (\vec{\nabla} \times \vec{B})_j, \quad (2)$$

where  $S$  denotes the deuteron spin, and  $\{.,.\}$  the anticommutator. Using Maxwell’s equations to replace the curl of the magnetic field with a current, we can trade the  $P\mathcal{T}$  moment for a contact interaction. For example, the  $P\mathcal{T}$  interaction of a non-relativistic lepton of mass  $m_l$  with the deuteron becomes a dimension-eight contact interaction,

$$V = \frac{e\mathcal{T}_d}{2m_l} \{S_i, S_j\} \left[ (\nabla_i \delta^{(3)}(\vec{x})) \hat{p}_j + \epsilon_{ikm} \sigma_k \nabla_m \nabla_j \delta^{(3)}(\vec{x}) \right]. \quad (3)$$

The first term is due to the lepton kinetic term and gives rise to a non-local interaction involving  $\hat{p} = -i\vec{\nabla}$ . The second one comes from the interaction of the lepton spin  $\vec{\sigma}$  with the deuteron  $P\bar{T}$  form factor. Effects of a TQFF on polarization observables in lepton-deuteron scattering have been investigated [7]. There should be similar effects in proton-deuteron scattering such as in the planned TRIC experiment at COSY [8], but there they are likely swamped by non-electromagnetic interactions.

We work in the framework of chiral effective field theory (EFT) and take into account the dominant parity and time-reversal violation in and beyond the Standard Model (SM) of particle physics.  $P$  violation is commonplace in the weak interaction of the SM.  $T$  violation, on the other hand, is small in the SM, which opens up the possibility that operators involving the SM fields but having dimension larger than four could be noticeable.  $T$  violation from the CKM quark-mixing matrix is suppressed with respect to other aspects of weak interactions by a small combination of matrix elements [9],  $J_{CP} \simeq 3 \cdot 10^{-5}$ . Moreover, it is loop suppressed in flavor-conserving quantities, such as  $T$ -violating form factors of the nucleon and nuclei. This leaves the QCD vacuum angle  $\bar{\theta}$  [10] as the potentially largest dimension-four source of such form factors. However, the stringent experimental limit on the neutron electric dipole moment,  $|d_n| < 2.9 \cdot 10^{-13} e \text{ fm}$  [11], constrains it to  $\bar{\theta} \lesssim 10^{-10}$ . Therefore, we also consider  $T$  violation originating beyond the SM at a high energy scale  $M_T$ . The dominant such higher-dimensional  $T$ -violating operators are of effective dimension six.

The TQFF is in principle sensitive to  $P\bar{T}$  physics beyond the SM. However, the lowest dimension where we find  $P\bar{T}$  operators is eight, which means that, in the simplest scenarios, they would be highly suppressed by the presumably high scale of physics beyond the SM. Discussions and references on  $P\bar{T}$  interactions at low energies, including situations where they could be relatively enhanced, can be found in Ref. [12]. We focus here on what is likely to be the largest “background” in the deuteron TQFF: the combination of  $\bar{P}T$  from the ordinary weak interactions with  $\bar{P}T$  from the  $\bar{\theta}$  term and from the dimension-six operators. Not surprisingly, we find a very small background value for the deuteron TQFF, so that any experimental evidence for a nonzero TQFF likely results from new  $P\bar{T}$  physics.

Our discussion is organized as follows. In Section 2 we construct the effective chiral Lagrangian for the relevant  $PT$ ,  $\bar{P}T$ , and  $\bar{P}\bar{T}$  interactions and currents involving nucleons, pions, and photons. In Section 3 we calculate the long-range contributions of these interactions to the deuteron TQFF. In Section 4 we discuss our results and compare the deuteron TQM to its  $\bar{P}\bar{T}$  electric dipole moment (EDM) and magnetic quadrupole moment (MQM). Three Appendices are devoted to details of our calculations. In Appendix A the various  $\bar{P}\bar{T}$  operators are presented in more detail, and the orders of magnitude of their contributions are given in Appendix B. In Appendix C we give the expansion of loop diagrams that define the deuteron TQFF.

## 2 The effective chiral Lagrangian

At a momentum  $Q$  much below the characteristic QCD scale,  $M_{\text{QCD}} \sim 1 \text{ GeV}$ , electromagnetic form factors can be calculated with low-energy effective field theories (EFTs). The most predictive such an EFT is chiral EFT (for a review, see Ref. [13]), a generalization to an arbitrary number of nucleons of chiral perturbation theory (ChPT) (for a review, see Ref. [14]), where  $Q \sim m_\pi$ , with  $m_\pi \simeq 140 \text{ MeV}$  the pion mass. In this EFT pion propagation is included explicitly, and the properties and interactions of the pions are strongly constrained by the approximate

chiral symmetry of QCD.

For the nucleon, form factors can be calculated in perturbation theory as a systematic expansion in  $Q/M_{\text{QCD}}$  [14]. The  $\cancel{P}T$  anapole and the  $\cancel{P}\cancel{T}$  electric dipole form factor of the nucleon have been calculated to next-to-leading order (NLO) in Refs. [15] and [16], respectively. In nuclei, pions can still be treated in perturbation theory [17], but then the expansion is in powers of  $Q/M_{NN}$ , where  $M_{NN} \equiv 4\pi F_\pi^2/m_N \sim F_\pi$  in terms of the pion decay constant  $F_\pi \simeq 186$  MeV. For observables involving momenta above  $M_{NN}$ , one-pion exchange needs to be iterated to all orders [18], which complicates renormalization [19]. However, light nuclei are dilute systems and, unless one is interested in form factors at high momentum, one can use a chiral EFT with perturbative pions. Indeed, the  $C$ -even electromagnetic form factors of the deuteron, both  $PT$  (charge, electric quadrupole, and magnetic dipole) [20] and  $\cancel{P}\cancel{T}$  (electric dipole and magnetic quadrupole) [21] have been successfully derived in this EFT. The TDDF of the deuteron has been calculated at LO in Ref. [22]. Similar calculations could be performed for other light nuclei.

The relevant low-energy EFT can be written in terms of nucleon, pion, and photon fields. The nucleon field  $N = (p \ n)^T$  is an isospinor bi-spinor, with isospin  $\tau/2$  and spin  $S^\mu = (0, \vec{\sigma}/2)$  in the rest frame, where the velocity is  $v^\mu = (1, \vec{0})$ . The pion field  $\pi$  is an isovector pseudoscalar, for which we choose a stereographic parametrization (see, *e.g.*, Ref. [23]) of the coset space  $SO(4)/SO(3)$ , where  $SU(2) \times SU(2) \sim SO(4)$  is the spontaneously broken, approximate chiral symmetry of QCD, and  $SU(2) \sim SO(3)$  its unbroken isospin subgroup. We define  $D \equiv 1 + \pi^2/F_\pi^2$ . The photon field  $A_\mu$  ensures electromagnetic  $U(1)$  gauge invariance, appearing in the gauge and chiral covariant derivatives  $D_\mu \pi_a = D^{-1}(\delta_{ab}\partial_\mu + e\epsilon_{3ab}A_\mu)\pi_b$  and  $\mathcal{D}_\mu N = [\partial_\mu + ieA_\mu(1 + \tau_3)/2 + i\tau \cdot (\pi \times D_\mu \pi)/F_\pi^2]N$ , and in the field strength  $F_{\mu\nu} = \partial_\mu A_\nu - \partial_\nu A_\mu$ . We use the notation  $\mathcal{D}_{\perp\pm}^\mu \equiv \mathcal{D}_\perp^\mu \pm \mathcal{D}_\perp^{\dagger\mu}$ , where  $\mathcal{D}_\perp^\mu = \mathcal{D}^\mu - v^\mu v \cdot \mathcal{D}$  and  $\bar{N}\mathcal{D}_\mu^\dagger = \overline{\mathcal{D}_\mu N}$ . The coefficients of interactions constructed with up to two nucleon fields are estimated, in the absence of other information from QCD, by naive dimensional analysis (NDA) [24]. For multi-nucleon couplings the scaling of a coefficient on the various scales depends also on the number of  $S$  waves the operator connects [17, 13].

In the following we will need only a few terms in the leading pion-nucleon-photon  $PT$  chiral Lagrangians, *viz.*

$$\begin{aligned} \mathcal{L}_{PT}^{(0)} = & \frac{1}{2}D_\mu \pi \cdot D^\mu \pi - \frac{m_\pi^2}{2D} \pi^2 + i\bar{N}v \cdot \mathcal{D}N - \frac{2g_A}{F_\pi}(D_\mu \pi) \cdot \bar{N}S^\mu \tau N \\ & - \frac{1}{2}C_0(\bar{N}N \bar{N}N - 4\bar{N}S^\mu N \cdot \bar{N}S_\mu N) + \dots, \end{aligned} \quad (4)$$

where  $g_A \simeq 1.27$  is the nucleon axial coupling and  $C_0$  a contact two-nucleon parameter, and

$$\begin{aligned} \mathcal{L}_{PT}^{(1)} = & -\frac{1}{2m_N}\bar{N}\mathcal{D}_\perp^2 N \\ & + \frac{e}{4m_N}\epsilon_{\rho\sigma\mu\nu}F^{\rho\sigma}v^\mu \bar{N} \left\{ 1 + \kappa_0 + (1 + \kappa_1) \left[ \tau_3 - \frac{2}{F_\pi^2 D} (\pi^2 \tau_3 - \pi_3 \pi \cdot \tau) \right] \right\} S^\nu N + \dots, \end{aligned} \quad (5)$$

where  $\kappa_0 \simeq -0.12$  and  $\kappa_1 \simeq 3.7$  are, respectively, the isoscalar and isovector anomalous magnetic moments of the nucleon, and  $\epsilon^{0123} = 1$ .

The  $P\cancel{T}$  TQFF vanishes unless there is, in the EFT, either a  $P\cancel{T}$  interaction or a combination of  $\cancel{P}T$  and  $\cancel{P}\cancel{T}$  interactions between the two nucleons.  $P\cancel{T}$  operators in the EFT Lagrangian

arise in two ways. First, they represent dimension-seven  $P\overline{T}$  operators in the quark-gluon Lagrangian just above  $M_{\text{QCD}}$ . These dimension-seven operators in turn can have two origins above the electroweak scale  $v$ . On one hand, they can be generated by possible gauge-invariant dimension-eight  $P\overline{T}$  operators, in which case they would be expected to be suppressed by four powers of the high, new-physics scale  $M_T$ , that is, they would scale as  $v/M_T^4$ . On the other hand, they can arise from the interplay of  $\not{P}T$  in the SM and possible dimension-six  $\not{P}\overline{T}$  operators, when one would expect the suppression scale to be  $v^2 M_T^2$  rather than  $M_T^4$ . A second way to generate  $P\overline{T}$  operators in the EFT Lagrangian is from  $\not{P}T$  and  $\not{P}\overline{T}$  interactions in the quark-gluon Lagrangian at low energy, when we integrate out non-perturbative dynamics on scale of order of the typical hadronic scale  $M_{\text{QCD}}$ . Again here we expect a suppression of  $v^2 M_T^2$  rather than  $M_T^4$ .

If the new-physics scale is much higher than the electroweak scale, the contributions from  $\not{P}T$  and  $\not{P}\overline{T}$  interactions are likely to dominate the  $P\overline{T}$  interactions in the EFT. Interesting scenarios in which this is not the case are discussed in Ref. [12]. Here we are interested in the background to genuine  $P\overline{T}$  interactions at the high energy scale. In this case, as discussed in App. B, the contributions from  $P\overline{T}$  interactions in the EFT are likely smaller than the long-range components from  $\not{P}T$  and  $\not{P}\overline{T}$  interactions, which we can, and will, calculate.

$\not{P}T$  interactions in chiral EFT have been discussed for example in Refs. [25, 26, 15]. They originate at the QCD scale from four-quark interactions proportional to the Fermi constant  $G_F \simeq 1.2 \cdot 10^{-5} \text{ GeV}^{-2}$ . A dimensionless measure of the relative strength of the weak interactions at low energies is  $G_F F_\pi^2 \sim 4 \cdot 10^{-7}$ . The most important interaction is the  $\not{P}T$  pion-nucleon interaction

$$\mathcal{L}_{\not{P}T}^{(-1)} = \frac{h_1}{F_\pi} \bar{N} (\boldsymbol{\pi} \times \boldsymbol{\tau})_3 N + \dots, \quad (6)$$

with  $h_1 = \mathcal{O}(G_F F_\pi^2 M_{\text{QCD}})$ . The  $\not{P}T$  pion-nucleon coupling  $h_1$  is not well-known. In LO of the EFT with perturbative pions, which we are employing, the  $\not{P}T$  asymmetry in  $n + p \rightarrow d + \gamma$  is  $A_\gamma = 0.24 h_1 / F_\pi$  [27], so the recent experimental result  $A_\gamma = [-1.2 \pm 2.1(\text{stat}) \pm 0.2(\text{sys})] \cdot 10^{-7}$  [28] gives a bound  $|h_1|/F_\pi \lesssim 10^{-6}$ , which is the order of magnitude expected by NDA. A first lattice QCD calculation at a pion mass  $m_\pi \simeq 389 \text{ MeV}$  gives, in our convention for  $h_1$ ,  $\sqrt{2} h_1 / F_\pi = [1.099 \pm 0.505_{-0.064}^{+0.058}] \cdot 10^{-7}$  [29].

$\not{P}\overline{T}$  interactions are expected to be due, mostly, to the dimension-four QCD  $\bar{\theta}$  term, parameterized by  $\bar{\theta} \ll 1$ , and the dimension-six operators that result from integrating out physics at the scale  $M_T$  and the heavy degrees of freedom in the SM. The complete set of  $\not{P}\overline{T}$  dimension-six operators at the electro-weak scale has been given in Ref. [30], and the relevant operators at the hadronic scale have been summarized in Ref. [31]. They are the isoscalar and isovector quark EDM (qEDM) and quark chromo-EDM (qCEDM), the Weinberg operator, which gives rise to a gluon chromo-EDM (gCEDM), and four  $\not{P}\overline{T}$  four-quark operators. Two of these four-quark operators are invariant under the SM gauge group and can be generated directly at the electroweak scale. Their effect in the chiral EFT at low energy cannot be separated from the gCEDM and we refer to these collectively as chiral-invariant sources ( $\chi$ ISs). The other two four-quark operators break isospin and result from integrating out the weak gauge bosons and running to low energy. Because they mix left- and right-handed quarks we denote these as FQLR. The various  $\not{P}\overline{T}$  sources are further discussed in App. A.

The dimension-four and six  $\not{P}\overline{T}$  operators have different transformation properties under the chiral group  $SU_L(2) \times SU_R(2)$ , which has consequences for the  $\not{P}\overline{T}$  couplings in chiral EFT

[32, 31]. The interactions relevant to the rest of the paper are

$$\begin{aligned}\mathcal{L}_{\mathcal{PT}} = & -\frac{\bar{g}_0}{F_\pi} \bar{N} \boldsymbol{\pi} \cdot \boldsymbol{\tau} N - \frac{\bar{g}_1}{F_\pi} \pi_3 \bar{N} N - 2\bar{N} (\bar{d}_0 + \bar{d}_1 \tau_3) S^\mu \left( v^\nu + \frac{i\mathcal{D}_{+-}^\nu}{2m_N} \right) N F_{\mu\nu} \\ & + \frac{1}{4} \bar{C}_0 [\bar{N} N \partial_\mu (\bar{N} S^\mu N) - \bar{N} \boldsymbol{\tau} N \cdot \mathcal{D}_\mu (\bar{N} S^\mu \boldsymbol{\tau} N)],\end{aligned}\quad (7)$$

where  $\bar{g}_0$  ( $\bar{g}_1$ ) is the isoscalar (isovector)  $\mathcal{PT}$  pion-nucleon coupling,  $\bar{d}_0$  ( $\bar{d}_1$ ) a short-range contribution to the isoscalar (isovector) nucleon EDM, and  $\bar{C}_0$  a short-range  $\mathcal{PT}$  two-nucleon interaction. The term proportional to  $1/m_N$  is a recoil correction and depends on the sum of the incoming and outgoing nucleon momenta. Other  $\mathcal{PT}$  interactions, some expected to be of comparable size, will not be needed below because of the quantum numbers of the deuteron.

The relative importance of the operators in Eq. (7) depends on the chiral properties of the  $\mathcal{PT}$  source at the quark-gluon level. As described in App. B, the dimensionless one-nucleon couplings  $\bar{g}_{0,1}/M_{\text{QCD}}$  and  $M_{\text{QCD}}\bar{d}_{0,1}/e$  are given by the dimensionless strengths of the underlying  $\mathcal{PT}$  interactions, times factors of  $(m_\pi/M_{\text{QCD}})^2$  that depend on the chiral transformation properties of the source. For the QCD  $\bar{\theta}$  term, the qCEDM, and the FQLR, which violate chiral symmetry, non-derivative pion-nucleon couplings like  $\bar{g}_0$  can appear in the chiral Lagrangian at LO. In this case  $\bar{g}_0/M_{\text{QCD}} = \mathcal{O}(M_{\text{QCD}}\bar{d}_1/e)$  and pion effects tend to dominate because of the low mass. In contrast,  $\chi$ ISs can generate pion-nucleon non-derivative couplings only through insertion of the quark mass, which costs two powers of  $m_\pi/M_{\text{QCD}}$ , so that, for example,  $\bar{g}_0/M_{\text{QCD}} = \mathcal{O}((m_\pi/M_{\text{QCD}})^2 M_{\text{QCD}}\bar{d}_1/e)$ . The  $\bar{g}_0$  term still appears in the LO Lagrangian, but it is accompanied by the equally important two-nucleon and electromagnetic operators, whose construction does not require any insertion of the quark mass. Finally, the presence of a photon field causes the qEDM to contribute mainly to the photon-nucleon sector, purely hadronic operators being suppressed by powers of  $\alpha_{\text{em}}/4\pi$ .

The interactions in Eqs. (6) and (7) can be used to compute the  $\mathcal{PT}$ ,  $\mathcal{PT}$  and  $P\mathcal{T}$  form factors of nuclei. The nucleon does not possess a  $P\mathcal{T}$  form factor. We summarize here the results for the nucleon TDFF and electric dipole form factor (EDFF), which are needed for the calculation of the deuteron TQFF in Sec. 3. The  $\mathcal{PT}$  and  $\mathcal{PT}$  currents are written as, respectively,

$$J_{\mathcal{PT}}^\mu(q) = \frac{2}{m_N^2} (F_{\mathcal{PT},0}(-q^2) + F_{\mathcal{PT},1}(-q^2)\tau_3) [S^\mu q^2 - S \cdot q q^\mu + \dots] \quad (8)$$

and

$$J_{\mathcal{PT}}^\mu(q, K) = 2i (F_{\mathcal{PT},0}(-q^2) + F_{\mathcal{PT},1}(-q^2)\tau_3) \left[ S^\mu \left( v \cdot q + \frac{K \cdot q}{m_N} \right) - S \cdot q \left( v^\mu + \frac{K^\mu}{m_N} \right) + \dots \right], \quad (9)$$

where  $q$  denotes the four-momentum of the photon and  $2K$  is the sum of the nucleon momenta. We write

$$F_{\mathcal{PT},i}(-q^2) = a_i f_i(-q^2/4m_\pi^2), \quad (10)$$

and

$$F_{\mathcal{PT},i}(-q^2) = d_i - q^2 S'_i(-q^2/4m_\pi^2), \quad (11)$$

where  $a_0$  and  $a_1$  ( $d_0$  and  $d_1$ ) are the nucleon isoscalar and isovector anapole (electric dipole) moments,  $f_i(0)=1$ , and  $S'_i(0)$  is finite.

At LO, the nucleon TDDFs come entirely from pion loops, in which one vertex is the  $\mathcal{PT}$  pion-nucleon coupling  $h_1$ . By NDA one expects  $a_i/m_N^2 = \mathcal{O}(eh_1/m_\pi M_{\text{QCD}}^2)$ . The calculation of Ref. [15] shows that the nucleon anapole form factor is, at LO, isoscalar and finite,

$$a_0^{(\text{LO})} = \frac{eg_A h_1 m_N^2}{24\pi F_\pi^2 m_\pi}, \quad f_0^{(\text{LO})}(x^2) = \frac{3}{2x^2} \left[ \frac{1+x^2}{x} \arctan x - 1 \right], \quad a_1^{(\text{LO})} = 0. \quad (12)$$

The isovector anapole form factor appears only at NLO, where short-range contributions to the moments also are present. Neglecting  $\mathcal{O}(1)$  numbers, the result (12) for  $a_0^{(\text{LO})}$  is a factor of  $4\pi$  larger than the NDA estimate, as often happens in baryon ChPT.

The nucleon EDFF was computed in Ref. [16] to NLO for all  $\mathcal{PT}$  sources of dimension up to six. For the QCD  $\bar{\theta}$  term, the qCEDM, and the FQLR, the isovector nucleon EDM receives a one-loop contribution from  $\bar{g}_0$  at LO. At the same order there are also short-range isoscalar ( $\bar{d}_0$ ) and isovector ( $\bar{d}_1$ ) contributions, the latter being required by renormalization-group invariance. The isoscalar and isovector nucleon EDMs are given by [33]

$$d_0^{(\text{LO})} = \bar{d}_0, \quad d_1^{(\text{LO})} = \bar{d}_1(\mu) + \frac{eg_A \bar{g}_0}{(2\pi F_\pi)^2} \left( L - \ln \frac{m_\pi^2}{\mu^2} \right), \quad (13)$$

where we used dimensional regularization in  $d$  spacetime dimensions, with  $L = 2/(4-d) - \gamma_E + \ln 4\pi$ , and  $\mu$  the renormalization scale. In this case there is no  $4\pi$  enhancement, and the nucleon EDM is suppressed by the loop factor  $(2\pi F_\pi)^2 \sim M_{\text{QCD}}^2$  with respect to the pion nucleon coupling  $\bar{g}_0$ . The momentum dependence of the EDFF is purely isovector in LO and governed by the scale  $m_\pi$ , as is the case for the isoscalar TDDF (12), but it is not needed in the following. For the qEDM and the  $\chi$ ISs,  $e\bar{g}_0/m_\pi^2$  is at most as large as the short-range coupling  $\bar{d}_1$ , and the loop suppression makes its contribution negligible. The EDFF is then momentum independent at LO and completely determined by the low-energy constants  $\bar{d}_{0,1}$ ,

$$d_{0,1}^{(\text{LO})} = \bar{d}_{0,1}, \quad S_{0,1}'^{(\text{LO})}(x^2) = 0. \quad (14)$$

In this case the momentum dependence appears in higher order and is determined by short-range physics.

The  $\mathcal{PT}$  couplings  $\bar{g}_0$ ,  $d_1$ , and  $\bar{C}_0$  are not known and, in order to estimate the magnitude of the TQFF they induce, we will need to make some reasonable assumptions. First, we assume that there are no cancellations between  $d_0^{(\text{LO})}$  and  $d_1^{(\text{LO})}$ , so that, for  $\mathcal{PT}$  violation from the qEDM and  $\chi$ ISs, the bound on the neutron EDM  $|d_n|$  can be directly translated into the bound  $|\bar{d}_1| < 2.9 \cdot 10^{-13} e \text{ fm}$ . Second, as pointed out in Ref. [33], we should not expect any cancellation in Eq. (13) between pieces that are non-analytic and analytic in  $m_\pi^2$ . With the reasonable value  $\mu = m_N$ , the same bound applies for  $|\bar{d}_1(m_N)|$  in the case of  $\bar{\theta}$  term, qCEDM and FQLR. Moreover, since the long-range contributions give the estimate  $|d_1| \sim 0.13(|\bar{g}_0|/F_\pi) e \text{ fm}$ , the existing experimental bound on the neutron EDM yields an approximate bound on the  $\mathcal{PT}$  pion-nucleon coupling,  $|\bar{g}_0|/F_\pi \lesssim 2 \cdot 10^{-12}$ .

### 3 TQFF of the deuteron

With the interactions described in Sec. 2, we can calculate the long-range contributions to the deuteron TQFF, using the techniques of Refs. [20, 22, 21]. As usual in such a calculation, the

orders of magnitude of the various contributions can be found by combining the power counting rules of ChPT based on NDA with the rules for two-nucleon states as summarized, for example, in Ref. [13]. A pion propagator scales as  $1/Q^2$ . A loop involving a single nucleon contributes a factor  $Q^4/(4\pi)^2$  from the integration and a factor  $1/Q$  from the nucleon propagator. The infrared enhancement of a loop involving two nucleons gives a factor  $Q^5/4\pi m_N$  from the integration and a factor  $m_N/Q^2$  from each nucleon propagator. The deuteron wavefunction contributes an overall normalization factor  $4\pi Q/m_N^2$ .

The deuteron itself is built out of the two-nucleon contact interaction with coefficient  $C_0 = \mathcal{O}(4\pi/m_N\gamma)$  and the nucleon kinetic terms in Eqs. (4) and (5). Pion exchange originating from the pion kinetic terms and pion-nucleon coupling in Eq. (4) contributes to the deuteron structure at relative  $\mathcal{O}(Q/M_{NN})$ , together with a two-derivative contact interaction that accounts for short-range energy dependence in the on-shell two-nucleon amplitude [17]. Since we calculate the TQFF to LO only,  $\gamma$  is the sole  $PT$  two-nucleon input needed.

The  $P\overline{T}$  TQFF is an intrinsically two-nucleon observable, which requires at least one symmetry-violating interaction between the two nucleons. We argue in App. B that  $P\overline{T}$  interactions are much smaller than contributions from separate  $\overline{P}T$  and  $\overline{P}\overline{T}$  interactions. The lowest-order diagrams involving the  $\overline{P}T$  vertex  $h_1$  and one of the  $\overline{P}\overline{T}$  couplings are shown in Figs. 1–3. In these figures, only one possible ordering is shown. Circles, triangles, and squares denote the leading  $PT$ ,  $\overline{P}T$ , and  $\overline{P}\overline{T}$  interactions in Eqs. (4), (6), and (7), respectively; a circled circle, the  $PT$  magnetic photon-nucleon interactions in Eq. (5); a twice circled triangle, the  $\overline{P}T$  anapole moment of the nucleon in Eq. (12). The hatched circles denote deuteron states obtained from the iteration of the leading two-nucleon interaction, which brings in dependence on the binding momentum  $\gamma$ . The natural scale for momentum dependence of the TQFF is  $4\gamma$ , so we express our results in terms of  $\vec{x} = \vec{q}/4\gamma$ . We also define the ratio  $\xi = \gamma/m_\pi$  of low-momentum scales.

Let us first consider a photon which interacts without breaking  $P$  and  $T$ . In this case the photon couples to the nucleon via the magnetic couplings in Eq. (5) or to a pion via interactions obtained by gauging the derivatives in the pion kinetic energy and pion-nucleon axial coupling in Eq. (4). Diagrams with only one pion exchange and  $\bar{g}_0$  and  $h_1$  vertices on each end vanish. This can be understood from the fact that such diagrams do not have enough powers of momentum in the vertices to generate a form factor of the form of Eq. (1), and it agrees with the more general analysis of the  $P\overline{T}$  two-nucleon interaction [34]. This leaves three-loop diagrams, containing either two pion exchanges (TPE) or one pion exchange and a short-range  $\overline{P}\overline{T}$  two-nucleon interaction (4N), Figs. 1 and 2 respectively. Using the power-counting rules outlined above, the sizes of the diagrams in Figs. 1 and 2 are

$$\text{Fig. 1} = \mathcal{O}\left(\frac{eh_1}{Q^2 M_{NN}^2} \frac{\bar{g}_0}{M_{\text{QCD}}}\right), \quad (15)$$

$$\text{Fig. 2} = \mathcal{O}\left(\frac{eh_1}{Q^2 M_{NN}^2} \frac{m_N \gamma \bar{C}_0}{4\pi} \frac{QM_{NN}}{M_{\text{QCD}}}\right). \quad (16)$$

Whether the diagrams in Figs. 1 or 2 are more important depends on the  $\overline{P}\overline{T}$  source. For the  $\bar{\theta}$  term, the qEDM, the qCEDM, and the FQLR operator the contributions from the short-range interaction  $\bar{C}_0$  are always suppressed, in this case by  $Q/M_{NN}$ , with respect to TPE, because for these sources  $\bar{g}_0 = \mathcal{O}(M_{NN}^2 m_N \gamma \bar{C}_0 / 4\pi)$ , see App. B. For  $\chi$ ISs, the opposite is true because of the extra  $(Q/M_{\text{QCD}})^2$  suppression of  $\bar{g}_0/M_{\text{QCD}}$ , which makes the short-range contributions larger by a factor of  $\mathcal{O}(M_{NN}/Q)$ . The diagrams in Fig. 1 are formally the leading contributions



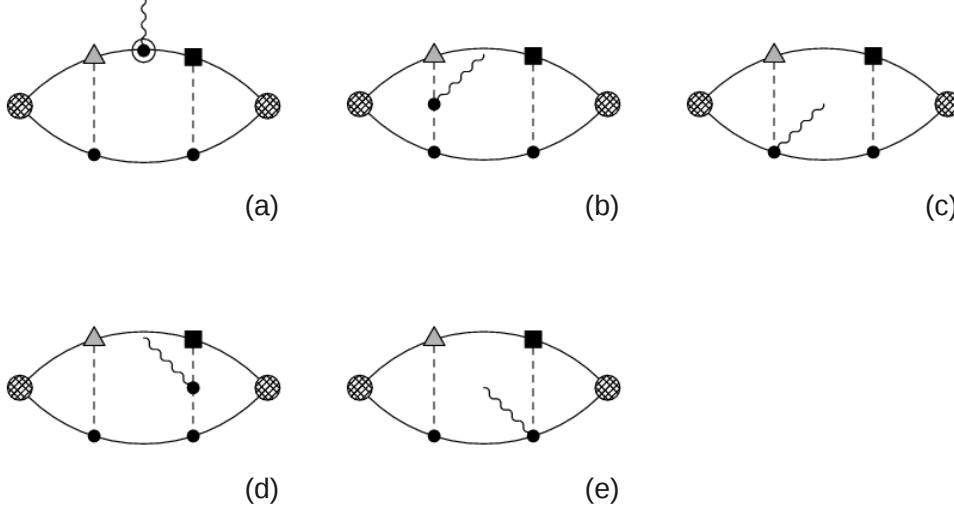


Figure 1: Two-pion-exchange (TPE) contributions to the deuteron TQFF,  $F_{PT}(\vec{q}^2)$ . Nucleons, pions and photons are represented by solid, dashed and wavy lines, respectively. LO  $PT$ ,  $\cancel{P}\cancel{T}$ , and  $\cancel{P}T$  interactions are denoted by circles, squares, and triangles, respectively. An NLO  $PT$  interaction is denoted by a circled circle. Deuteron states obtained from the iteration of the leading  $PT$  two-nucleon interaction are represented by hatched circles.

for the QCD  $\bar{\theta}$  term, the qCEDM, and the FQLR, while those in Fig. 2 are leading for the  $\chi$ ISs. Note that for the isovector qCEDM and the FQLR, one should consider not only the isoscalar pion-nucleon coupling  $\bar{g}_0$  but also the isovector pion-nucleon coupling  $\bar{g}_1$ , but such diagrams vanish.

Alternatively, the photon can interact with the nucleon with a  $\cancel{P}T$  or  $\cancel{P}\cancel{T}$  interaction, in which case a single two-nucleon interaction,  $\cancel{P}\cancel{T}$  or  $\cancel{P}T$  respectively, is sufficient to produce a TQFF — see Fig. 3. In diagrams 3(a,b) one of the nucleons couples to the magnetic field via its anapole moment, with  $\cancel{P}\cancel{T}$  coming either from pion exchange or from a two-nucleon interaction. Here the anapole “vertex” stands for a one-loop diagram, which produces the result (12). In diagram 3(c) the photon couples to the nucleon through a recoil correction to the  $\cancel{P}\cancel{T}$  EDM, with  $\cancel{P}T$  coming from pion exchange. By power counting, the contributions of diagrams 3(a,b) to the TQFF are

$$\text{Fig. 3(a)} = \mathcal{O}\left(\frac{a_i}{m_N^2} \frac{\bar{g}_0}{QM_{NN}}\right) = \mathcal{O}\left(\frac{eh_1}{Q^2 M_{NN}^2} \frac{\bar{g}_0 M_{NN}}{M_{\text{QCD}}^2}\right), \quad (17)$$

$$\text{Fig. 3(b)} = \mathcal{O}\left(\frac{a_i}{m_N^2} \frac{m_N \gamma \bar{C}_0}{4\pi}\right) = \mathcal{O}\left(\frac{eh_1}{Q^2 M_{NN}^2} \frac{m_N \gamma \bar{C}_0}{4\pi} \frac{QM_{NN}^2}{M_{\text{QCD}}^2}\right), \quad (18)$$

were we used the NDA expectation for the anapole moment. Diagrams 3(a,b) are thus suppressed by one power of  $M_{NN}/M_{\text{QCD}} \sim 1/4\pi$  compared to the contributions of Figs. 1 and 2. However,  $a_0$  in Eq. (12) is a factor of  $4\pi$  larger than the NDA estimate, making the corresponding contributions to the TQFF competitive with LO. Again, of other possible  $\cancel{P}\cancel{T}$  couplings only

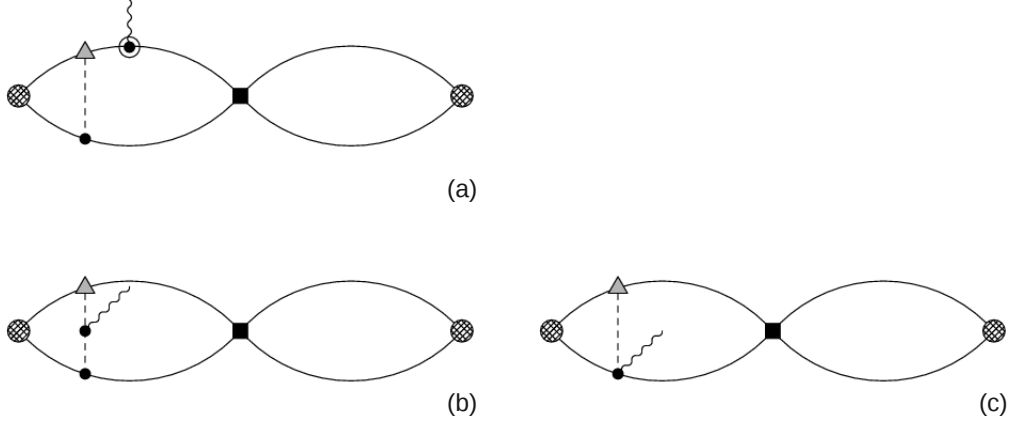


Figure 2: Short-range two-nucleon ( $4N$ ) contributions to the deuteron TQFF,  $F_{PT}(\vec{q}^2)$ . The notation is as in Fig. 1.

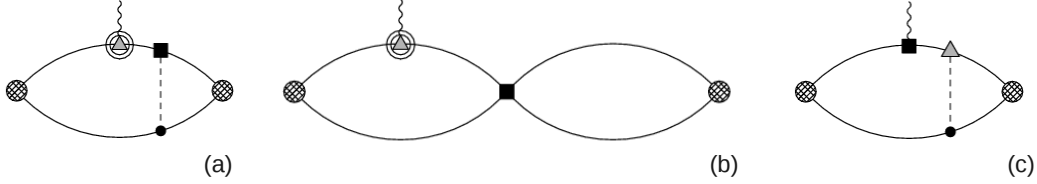


Figure 3: Nucleon anapole form factor (TDFF) and electric dipole moment (EDM) contributions to the deuteron TQFF,  $F_{PT}(\vec{q}^2)$ . The twice-circled triangle stands for the anapole form factor. The other notation is as in Fig. 1.

$\bar{g}_0$  and  $\bar{C}_0$  contribute. Diagram 3(c) represents contributions to the TQFF coming from the nucleon EDFF. It scales as

$$\text{Fig. 3(c)} = \mathcal{O}\left(\frac{eh_1}{Q^2 M_{NN}^2} \frac{\bar{d}_1}{e} \frac{QM_{NN}}{M_{\text{QCD}}}\right), \quad (19)$$

and there is no contribution from  $\bar{d}_0$  at this order. For  $\bar{\theta}$  term, qCEDM, and FQLR,  $\bar{d}_1/e = \mathcal{O}(\bar{g}_0/M_{\text{QCD}}^2)$  and this contribution is suppressed by  $Q/M_{\text{QCD}}$  (a factor coming from the recoil) compared to the analogous anapole diagram 3(a). For  $\chi$ ISs, this contribution is comparable to Fig. 2, while for the qEDM it is the sole leading contribution, since numerically  $\alpha_{\text{em}}/4\pi \sim (Q/M_{\text{QCD}})^3$ .

To summarize these power-counting arguments, we expect the TQFF induced by the  $\bar{\theta}$  term, the qCEDM, and the FQLR to be dominated by the TPE diagrams in Fig. 1, with possibly large corrections from the nucleon TDFF, diagram 3(a). For  $\chi$ ISs, the dominant contribution should come from the diagrams involving the  $P/T$  short-range two-nucleon interaction in Fig. 2 and from the nucleon EDFF, diagram 3(c), with a sizable correction from the nucleon TDFF, diagram 3(b). For the qEDM only the nucleon EDFF contribution 3(c) should be important.

We now proceed to the evaluation of diagrams in Figs. 1, 2, and 3. We find that only the isovector magnetic moment gives a non-vanishing contribution to diagram 1(a) and 2(a). Diagrams with other photon-nucleon interactions (the isoscalar magnetic moment and the minimal coupling through the covariant derivative in the nucleon kinetic term) vanish. Similar diagrams where pion exchanges and contact interaction occur both before or after the insertion of the photon coupling also vanish. Diagrams 1(b,c) and 1(d,e) differ only by an isospin factor.

The diagrams in Fig. 1 are finite in four (and three) dimensions. We express the result for their contribution to the TQFF as

$$F_{PT}^{(\text{TPE})}(\vec{q}^2) = -\frac{eg_A^2\bar{g}_0h_1}{m_\pi^2} \frac{m_N}{(4\pi F_\pi^2)^2} \left[ (1 + \kappa_1) I_a^{(3)}\left(\frac{\gamma}{m_\pi}, \frac{\vec{q}}{4\gamma}\right) + I_b^{(3)}\left(\frac{\gamma}{m_\pi}, \frac{\vec{q}}{4\gamma}\right) \right], \quad (20)$$

in terms of two three-loop integrals  $I_{a,b}^{(3)}(\xi, \vec{x})$ . Likewise, the results for the TQFF in Fig. 2 are expressed in terms of two two-loop functions  $I_{a,b}^{(2)}(\xi, \vec{x})$  as

$$F_{PT}^{(4N)}(\vec{q}^2) = \frac{eg_Ah_1}{m_\pi} \frac{m_N}{4\pi F_\pi^2} \frac{\mu - \gamma}{4\pi} \bar{C}_0 \left[ (1 + \kappa_1) I_a^{(2)}\left(\frac{\gamma}{m_\pi}, \frac{\vec{q}}{4\gamma}\right) + I_b^{(2)}\left(\frac{\gamma}{m_\pi}, \frac{\vec{q}}{4\gamma}\right) \right], \quad (21)$$

where we have used power-divergence subtraction [17]. The  $\mu$  dependence is absorbed in  $\bar{C}_0$  itself, since here it appears in the same combination as in the magnetic quadrupole form factor [21]. The expansions to order  $\vec{q}^2$  of the integrals  $I_{a,b}^{(2,3)}$  are given in App. C. The resulting contributions to the TQM are

$$\mathcal{T}_d^{(\text{TPE})} \simeq [0.8(1 + \kappa_1) - 0.9] \cdot 10^{-2} \frac{\bar{g}_0h_1}{F_\pi^2} e \text{ fm}^3. \quad (22)$$

and

$$\mathcal{T}_d^{(4N)} \simeq [1.0(1 + \kappa_1) - 0.7] \cdot 10^{-2} m_N \frac{\mu - \gamma}{4\pi} \bar{C}_0 h_1 e \text{ fm}^3. \quad (23)$$

Finally, we consider diagrams 3(a,b) and (c). For isoscalar  $\mathcal{PT}$ , only the isoscalar TDFF  $F_{\mathcal{PT},0}$  contributes in diagrams 3(a,b). Isospin-breaking  $\mathcal{PT}$ , for example from insertions of  $\bar{g}_1$ , would contribute to diagram 3(a) together with the isovector TDFF  $F_{\mathcal{PT},1}$ . However, the isovector TDFF is suppressed by  $Q/M_{\text{QCD}}$  (and by a factor of  $4\pi$ ) with respect to the isoscalar TDFF. Therefore, even for sources that generate  $\bar{g}_0$  and  $\bar{g}_1$  at the same level,  $\bar{g}_1$  contributions to the TQFF are subleading. Diagram 3(c) is leading only for the qEDM and  $\chi$ ISs, for which the isovector EDFF is momentum independent and coincides with the EDM. Diagrams 3(a,b) and (c) result in contributions to the TQFF given by

$$F_{PT}^{(\text{TDFF})}(\vec{q}^2) = \frac{F_{\mathcal{PT},0}(\vec{q}^2)}{4\pi m_N} \left[ \frac{g_A\bar{g}_0}{m_\pi F_\pi^2} I_c^{(2)}\left(\frac{\gamma}{m_\pi}, \frac{\vec{q}}{4\gamma}\right) + (\mu - \gamma) \bar{C}_0 I^{(1)}\left(\frac{\vec{q}}{4\gamma}\right) \right] \quad (24)$$

and

$$F_{PT}^{(\text{EDM})}(\vec{q}^2) = \frac{g_A}{4\pi F_\pi^2 m_\pi} h_1 \bar{d}_1 I_d^{(2)}\left(\frac{\gamma}{m_\pi}, \frac{\vec{q}}{4\gamma}\right), \quad (25)$$

respectively. The expression for the one-loop integral  $I^{(1)}$  along with the expansions to order  $\vec{q}^2$  of two-loop integrals  $I_{c,d}^{(2)}$  can be found in App. C. Numerically this gives

$$\mathcal{T}_d^{(\text{TDFF})} \simeq \left[ 3.5 \frac{\bar{g}_0}{F_\pi^2} + 2.7 m_N \frac{\mu - \gamma}{4\pi} \bar{C}_0 \right] \cdot 10^{-2} h_1 e \text{ fm}^3 \quad (26)$$

and

$$\mathcal{T}_d^{(\text{EDM})} \simeq 1.3 \cdot 10^{-2} \bar{d}_1 h_1 \text{ fm}^3. \quad (27)$$

The result (26) shows that the TDFF contribution, though expected to be suppressed by the factor  $M_{NN}/M_{\text{QCD}}$ , is comparable to the LO values in Eqs. (22) and (23), in line with the  $4\pi$  enhancement in the TDM. For the QCD  $\bar{\theta}$  term, the qCEDM, and the FQLR, we can assess the importance of the EDM contribution to the TQFF by substituting in Eq. (27) the estimate for the nucleon EDM in terms of  $\bar{g}_0$ ,  $|d_1| \sim 0.13(|\bar{g}_0|/F_\pi) e \text{ fm}$ . We find  $\mathcal{T}_d^{(\text{EDM})} \sim 0.2 \cdot 10^{-2} (\bar{g}_0 h_1 / F_\pi^2) e \text{ fm}^3$ , which is numerically small compared to Eqs. (22) and (26), as expected by power counting.

We can now combine the results found so far. For the QCD  $\bar{\theta}$  term, the qCEDM, and the FQLR, the TPE contributions from the diagrams in Fig. 1 and the TDFF contributions in Fig. 3(a) have comparable size, giving

$$(\mathcal{T}_d)_{\bar{\theta}, \text{qCEDM}, \text{FQLR}} \simeq 6.3 \cdot 10^{-2} \frac{\bar{g}_0 h_1}{F_\pi^2} e \text{ fm}^3. \quad (28)$$

This number is within a factor  $\simeq 2$  of the power counting estimate in Eq. (17), indicating that the power counting works well (apart from the  $4\pi$  in the anapole moment).

For  $\chi$ ISs, by power counting the leading contributions are expected to come from the diagrams in Fig. 2, with insertions of the four-nucleon coupling  $\bar{C}_0$ , and from the EDM in diagram 3(c). Also in this case, the contribution of the TDFF in diagram 3(b) is numerically important. We find

$$(\mathcal{T}_d)_{\chi\text{ISs}} \simeq \left[ 6.7 m_N \frac{\mu - \gamma}{4\pi} \bar{C}_0 + 1.3 \frac{\bar{d}_1}{e} \right] \cdot 10^{-2} h_1 e \text{ fm}^3. \quad (29)$$

If  $\bar{C}_0$  and  $\bar{d}_1$  have their NDA values, their respective contributions are numerically comparable.

In the case of the qEDM, the TQM is dominated by the contribution from the nucleon EDM, and we find

$$(\mathcal{T}_d)_{\text{qEDM}} \simeq 1.3 \cdot 10^{-2} \bar{d}_1 h_1 \text{ fm}^3. \quad (30)$$

Because of dimensionless numerical factors this value is about an order of magnitude smaller than expected by the power-counting estimates based on NDA.

## 4 Discussion and conclusion

It is interesting to compare our results for the deuteron TQM in Eqs. (28), (29), and (30) with the largest  $\mathcal{PT}$  moment of the deuteron, EDM or MQM, for the respective  $\mathcal{PT}$  sources. In Ref. [21] power-counting estimates and LO results were given for the deuteron EDM,  $d_d$ , and MQM,  $\mathcal{M}_d$ , in chiral EFT with perturbative pion exchange.

For sources that break chiral symmetry and generate non-derivative  $\mathcal{PT}$  pion-nucleon couplings in LO,  $d_d$  and  $\mathcal{M}_d$  are expected to be dominated by two-body effects and be enhanced with respect to the nucleon EDM. In the case of the QCD  $\bar{\theta}$  term,  $\mathcal{M}_d$  is expected to be the largest moment (in natural units), because at LO  $\bar{g}_0$  does not contribute to  $d_d$  (except through the nucleon EDM, Eq. (13)). On the other hand, the qCEDM and the FQLR, which generate also the isovector coupling  $\bar{g}_1$  in LO, induce  $d_d$  and  $\mathcal{M}_d$  of the same size. For  $\chi$ ISs,  $d_d$  and  $\mathcal{M}_d$  are also expected to be of the same size, and of similar size as the nucleon EDM. The deuteron EDM is in fact expected to be well approximated by (twice) the isoscalar nucleon EDM, while

the deuteron MQM, in the perturbative-pion counting, receives the largest contribution from the four-nucleon coupling  $\bar{C}_0$ . For all these sources, we compare the deuteron TQM to its MQM, given by [21]

$$\mathcal{M}_d = \frac{eg_A\bar{g}_0}{m_\pi} \frac{1}{2\pi F_\pi^2} \left[ (1 + \kappa_0) + \frac{\bar{g}_1}{3\bar{g}_0}(1 + \kappa_1) \right] \frac{1 + \xi}{(1 + 2\xi)^2} + e(1 + \kappa_0) \frac{\mu - \gamma}{2\pi} \bar{C}_0. \quad (31)$$

We consider the dimensionless ratio  $F_\pi \mathcal{T}_d / \mathcal{M}_d$ , which, by power counting, is expected to be of order  $h_1 / F_\pi$ .

For the  $\bar{\theta}$  term, qCEDM, and FQLR,  $\bar{C}_0$  is subleading in Eq. (31), so that from Eq. (28)

$$F_\pi \left| \frac{\mathcal{T}_d}{\mathcal{M}_d} \right|_{\bar{\theta}, \text{qCEDM}, \text{FQLR}} \simeq 0.4 \left| \frac{\bar{g}_0}{\bar{g}_0 + 1.8\bar{g}_1} \right| \frac{|h_1|}{F_\pi}. \quad (32)$$

For the  $\bar{\theta}$  term, one can neglect  $\bar{g}_1$  and the  $\mathcal{PT}$  couplings drop out of the ratio, which is approximately  $|h_1|/F_\pi$ , as expected by power counting. For the qCEDM the ratio in Eq. (32) depends on  $|\bar{g}_0/\bar{g}_1|$ , which by NDA is expected to be order one. For the FQLR, as discussed in Ref. [31],  $\bar{g}_0$  is somewhat suppressed with respect to  $\bar{g}_1$ , further suppressing the deuteron TQM with respect to the MQM. In the case of  $\chi$ ISs,  $\bar{C}_0$  is expected to be the leading term in Eq. (31); if we neglect the contribution of the nucleon EDM in Eq. (29), we get

$$F_\pi \left| \frac{\mathcal{T}_d}{\mathcal{M}_d} \right|_{\chi\text{IS}} \simeq 0.2 \frac{|h_1|}{F_\pi}, \quad (33)$$

which is also in good agreement with the NDA expectation.

For the remaining dimension-six source, the qEDM,  $d_d$  is also well approximated by the isoscalar nucleon EDM,

$$d_d = 2\bar{d}_0, \quad (34)$$

while  $\mathcal{M}_d$  is suppressed by one power of  $Q/M_{NN}$  with respect to the EDM [21]. Therefore, for the qEDM we compare the deuteron TQM with its EDM using the dimensionless ratio  $m_N F_\pi \mathcal{T}_d / d_d$ . From Eq. (30),

$$m_N F_\pi \left| \frac{\mathcal{T}_d}{d_d} \right|_{\text{qEDM}} \simeq 0.03 \left| \frac{\bar{d}_1}{\bar{d}_0} \right| \frac{|h_1|}{F_\pi}, \quad (35)$$

which is a bit smaller than naively expected.

Equations (32), (33) and (35) make it explicit that the deuteron TQFF, in natural units, is suppressed roughly by a factor of  $h_1/F_\pi \sim G_F M_{\text{QCD}}^2 / 4\pi \sim 10^{-6}$  with respect to the largest  $\mathcal{PT}$  moment. The lack of any significant numerical enhancement thus leads to a very small TQFF. The bounds on  $\bar{g}_0$ ,  $\bar{d}_1$ , and  $h_1$  inferred in Sec. 2 allow us to estimate the size of the TQM. For the QCD  $\bar{\theta}$  term, the qCEDM, and the FQLR we find

$$|\mathcal{T}_d|_{\bar{\theta}, \text{qCEDM}, \text{FQLR}} \lesssim 1.2 \cdot 10^{-19} \text{ e fm}^3, \quad (36)$$

while for the qEDM we find the even smaller value

$$|\mathcal{T}_d|_{\text{qEDM}} \lesssim 3.5 \cdot 10^{-21} \text{ e fm}^3. \quad (37)$$

For  $\chi$ ISs, one expects a similar value, but to be more precise a bound on  $\bar{C}_0$  is needed.

These estimates have been obtained in chiral EFT with perturbative pions. Iterating pions one can extend the regime of validity of the theory beyond  $M_{NN}$  at the cost of much more complicated renormalization [19]. Because the binding momentum of nucleons in the deuteron is  $\gamma \ll M_{NN}$ , we do not expect drastic changes in the quantities calculated here. In the case of our comparison  $\mathcal{PT}$  moments, this expectation has been checked [35] and shown to be reasonable.

We conclude that the value of the deuteron TQM from parity violation in the SM and parity- and time-reversal violation due to the SM  $\bar{\theta}$  term or dimension-six operators originating beyond the SM is, not surprisingly, tiny. Evidence for a nonzero value for the deuteron TQM that is larger than the “background” value  $\sim 10^{-19} \text{ e fm}^3$  would likely be due to new  $\mathcal{PT}$  interactions.

## Acknowledgements

U. van Kolck acknowledges the hospitality of the KVI Groningen on many occasions. This research was supported by the Dutch Stichting FOM under programs 104 and 114 (JdV, RGET) and in part by the DFG and the NSFC through funds provided to the Sino-German CRC 110 “Symmetries and the Emergence of Structure in QCD” (JdV), by the US DOE under contract DE-AC02-05CH11231 with the Director, Office of Science, Office of High Energy Physics (EM), and under grant DE-FG02-04ER41338 (UvK), and by the Université Paris Sud under the program Attractivité 2013 (UvK).

## Appendices

### A Dimension-six operators

The  $\mathcal{PT}$  operators of dimension four and six, after integrating out physics at the scale  $M_T$  and the heavy degrees of freedom in the SM, are given by [31]

$$\begin{aligned} \mathcal{L}_{\mathcal{PT}} = & m_\star \bar{\theta} \bar{q} i \gamma_5 q - \frac{1}{2} \bar{q} (d_0 + d_3 \tau_3) i \sigma^{\mu\nu} \gamma_5 q F_{\mu\nu} - \frac{1}{2} \bar{q} (\tilde{d}_0 + \tilde{d}_3 \tau_3) i \sigma^{\mu\nu} \gamma_5 \lambda^a q G_{\mu\nu}^a \\ & + \frac{d_W}{6} f^{abc} \epsilon^{\mu\nu\alpha\beta} G_{\alpha\beta}^a G_{\mu\rho}^b G_\nu^c \\ & + \frac{\text{Im} \Xi_1}{4} \epsilon^{3ij} \bar{q} \tau^i \gamma^\mu q \bar{q} \tau^j \gamma_\mu \gamma_5 q + \frac{\text{Im} \Xi_8}{4} \epsilon^{3ij} \bar{q} \tau^i \gamma^\mu \lambda^a q \bar{q} \tau^j \gamma_\mu \lambda^a \gamma_5 q \\ & + \frac{\text{Im} \Sigma_1}{4} (\bar{q} q \bar{q} i \gamma_5 q - \bar{q} \boldsymbol{\tau} q \cdot \bar{q} \boldsymbol{\tau} i \gamma_5 q) + \frac{\text{Im} \Sigma_8}{4} (\bar{q} \lambda^a q \bar{q} i \gamma_5 \lambda^a q - \bar{q} \boldsymbol{\tau} \lambda^a q \cdot \bar{q} \boldsymbol{\tau} i \gamma_5 \lambda^a q). \end{aligned} \quad (38)$$

The first operator is the QCD  $\bar{\theta}$  term, where  $m_\star$  denotes the reduced light-quark mass  $m_\star = m_u m_d / (m_u + m_d)$ . We assume that  $\bar{\theta} \ll 1$ . In the second and third operators,  $d_0$  ( $d_3$ ) and  $\tilde{d}_0$  ( $\tilde{d}_3$ ) are the isoscalar (isovector) components of the quark EDM (qEDM) and quark chromo-EDM (qCEDM), respectively. In the fourth term,  $d_W$  represents the gluon chromo-EDM (gCEDM). The remainder consists of  $\mathcal{PT}$  four-quark operators. The ones with coefficients  $\Sigma_{1,8}$  are invariant under the SM gauge group, and can be generated directly at the electroweak scale. The isospin-breaking four-quark operators (FQLR) with coefficients  $\Xi_{1,8}$ , on the other hand, are generated by integrating out the weak gauge bosons and running to low energy.

The importance of the dimension-six  $\mathcal{PT}$  operators depends on the high energy scale  $M_T$ , on the detailed mechanism of  $P$  and  $T$  breaking in new physics, and on the running to the QCD

scale (for the latter, see Ref. [36] and references therein). We hide all the model dependence by introducing the dimensionless parameters  $\delta_{0,3}$ ,  $\tilde{\delta}_{0,3}$ ,  $w$ ,  $\xi$ , and  $\sigma_{1,8}$  for (isoscalar and isovector) qEDM and qCEDM, gCEDM, and isospin-breaking and invariant four-quark operators, respectively. We write [31]

$$\begin{aligned} d_{0,3} &= \mathcal{O}\left(\frac{e\delta_{0,3}\bar{m}}{M_T^2}\right), & \tilde{d}_{0,3} &= \mathcal{O}\left(4\pi\frac{\tilde{\delta}_{0,3}\bar{m}}{M_T^2}\right), & d_W &= \mathcal{O}\left(4\pi\frac{w}{M_T^2}\right), \\ \Xi_{1,8} &= \mathcal{O}\left(\frac{(4\pi)^2\xi}{M_T^2}\right), & \Sigma_{1,8} &= \mathcal{O}\left(\frac{(4\pi)^2\sigma_{1,8}}{M_T^2}\right). \end{aligned} \quad (39)$$

Naively, one expects  $\delta_{0,3}$ ,  $\tilde{\delta}_{0,3}$ ,  $w$ ,  $\xi$ , and  $\sigma_{1,8}$  to be  $\mathcal{O}(1)$ ,  $\mathcal{O}(g_s/4\pi)$ ,  $\mathcal{O}((g_s/4\pi)^3)$ ,  $\mathcal{O}(1)$ , and  $\mathcal{O}(1)$ , respectively, but they could be significantly smaller or larger, depending on the new-physics model. As in the case of electroweak interactions, the relative strength of  $\mathcal{P}\mathcal{T}$  interactions at low energies is expressed by the ratio of a low-energy scale and the characteristic scale where  $P$  and  $T$  violation arise. The dimension-four  $\bar{\theta}$  term is not suppressed by any high energy scale, and its reduced coupling is  $\bar{\theta}m_\pi^2/M_{\text{QCD}}^2$ , where the pion mass is a reminder of the intimate relationship between the  $\bar{\theta}$  term and the quark masses. In the case of dimension-six operators, the qEDM and qCEDM require an insertion of the Higgs vacuum expectation value, which can be traded for the quark mass. A dimensionless measure of their importance is then  $(\tilde{\delta}_{0,3}, \delta_{0,3})m_\pi^2/M_T^2$ . For the remaining dimension-six  $\mathcal{P}\mathcal{T}$  operators the relevant low energy scale is  $M_{\text{QCD}}$ , and the reduced couplings are  $(w, \sigma_{1,8}, \xi)M_{\text{QCD}}^2/M_T^2$ .

## B Orders of magnitude

In terms of the dimensionless parameters defined in App. A, we can estimate [32, 31] the size of the couplings  $\bar{g}_0$  and  $\bar{d}_1$  in Eq. (7) using NDA as

$$\bar{g}_0 = \mathcal{O}\left(\bar{\theta}\frac{m_\pi^2}{M_{\text{QCD}}}, (\tilde{\delta}_0, \varepsilon\tilde{\delta}_3)\frac{m_\pi^2 M_{\text{QCD}}}{M_T^2}, \varepsilon\xi\frac{M_{\text{QCD}}^3}{M_T^2}, (w, \sigma_{1,8})\frac{m_\pi^2 M_{\text{QCD}}}{M_T^2}, \delta_{0,3}\frac{\alpha_{\text{em}}}{4\pi}\frac{m_\pi^2 M_{\text{QCD}}}{M_T^2}\right) \quad (40)$$

$$\frac{\bar{d}_1}{e} = \mathcal{O}\left(\bar{\theta}\frac{m_\pi^2}{M_{\text{QCD}}^3}, \tilde{\delta}_{0,3}\frac{m_\pi^2}{M_{\text{QCD}}M_T^2}, \xi\frac{M_{\text{QCD}}}{M_T^2}, (w, \sigma_{1,8})\frac{M_{\text{QCD}}}{M_T^2}, (\varepsilon\delta_0\frac{m_\pi^2}{M_{\text{QCD}}}, \delta_3)\frac{m_\pi^2}{M_{\text{QCD}}M_T^2}\right) \quad (41)$$

Here  $\varepsilon$  is related to the light quark mass difference by  $m_d - m_u \equiv \varepsilon(m_u + m_d)$ . In the case of the QCD  $\bar{\theta}$  term, chiral symmetry relates  $\bar{g}_0$  to the strong contribution to the neutron-proton mass difference by [33, 32]  $\bar{g}_0 = \delta m_N(1 - \varepsilon^2)\bar{\theta}/2\varepsilon \simeq 3\bar{\theta}$  MeV, using results from a lattice QCD calculation [37]. For the dimension-six operators, going beyond NDA requires additional input from lattice QCD or other non-perturbative techniques. The contributions to  $\bar{g}_0$  from the isovector component of the qCEDM and the FQLR, which break isospin, are suppressed by the quark-mass difference. These two sources, as well as the  $\chi$ ISs, generate at leading order also the isovector pion-nucleon coupling  $\bar{g}_1$ . However, as we discuss in the main text, such a coupling does not contribute to the TQFF at LO. For all sources there is also an isoscalar EDM component  $\bar{d}_0$ , but this term is not relevant here either.

The estimate of the LEC  $\bar{C}_0$  associated with the four-nucleon operator in Eq. (7) requires more care [21, 38]. In the EFT where pion exchange is treated perturbatively, pions with momentum

above  $M_{NN}$  are integrated out, which induces contributions to multi-nucleon interactions. In particular,  $\bar{C}_0$  can be generated by a high-energy pion exchange between two nucleons with one vertex originating in  $g_A$  and the other in  $\bar{g}_0$ . For  $\chi$ ISs a larger contribution to  $\bar{C}_0$  is generated if one uses, instead of  $\bar{g}_0$ ,  $(\bar{\zeta}_1/F_\pi)(D^2\pi) \cdot \bar{N}\tau N$ , where  $\bar{\zeta}_1 = \mathcal{O}((w, \sigma_{1,8})M_{\text{QCD}}/M_T^2)$  [31]. Application of the NDA rules at the scale  $M_{NN}$  then gives  $\bar{C}_0 = \mathcal{O}(g_A\bar{g}_0 4\pi/m_N M_{NN}^3)$  or  $\bar{C}_0 = \mathcal{O}(g_A\bar{\zeta}_1 4\pi/m_N M_{NN})$ . However, this naive scaling is altered because the operator connects to an  $S$  wave. As discussed in Ref. [17], this enhances the scaling by a factor  $M_{NN}/Q$  due to non-perturbative renormalization by the leading-order  $PT$  two-nucleon interaction. One finds

$$\frac{m_N\gamma}{4\pi}\bar{C}_0 = \mathcal{O}\left(\bar{\theta}\frac{m_\pi^2}{M_{NN}^2 M_{\text{QCD}}}, (\tilde{\delta}_0, \varepsilon\delta_3)\frac{m_\pi^2 M_{\text{QCD}}}{M_{NN}^2 M_T^2}, \xi\frac{M_{\text{QCD}}^3}{M_{NN}^2 M_T^2}, (w, \sigma_{1,8})\frac{M_{\text{QCD}}}{M_T^2}, \delta_{0,3}\frac{\alpha_{\text{em}}}{4\pi}\frac{m_\pi^2 M_{\text{QCD}}}{M_{NN}^2 M_T^2}\right). \quad (42)$$

Combining the scaling of these low-energy constants with the power-counting rules outlined in Sec. 3, we find for the size of the diagrams in Figs. 1, 2, and 3:

$$\begin{aligned} \text{Fig. 1} &= \mathcal{O}\left(\frac{eG_F}{4\pi M_{NN}}\right) \times \\ &\mathcal{O}\left(\bar{\theta}, (\tilde{\delta}_0, \varepsilon\tilde{\delta}_3)\frac{M_{\text{QCD}}^2}{M_T^2}, \varepsilon\xi\frac{M_{\text{QCD}}^4}{Q^2 M_T^2}, (w, \sigma_{1,8})\frac{M_{\text{QCD}}^2}{M_T^2}, \delta_{0,3}\frac{\alpha_{\text{em}}}{4\pi}\frac{M_{\text{QCD}}^2}{M_T^2}\right), \end{aligned} \quad (43)$$

$$\begin{aligned} \text{Fig. 2} &= \mathcal{O}\left(\frac{eG_F Q}{4\pi M_{NN}^2}\right) \times \\ &\mathcal{O}\left(\bar{\theta}, (\tilde{\delta}_0, \varepsilon\tilde{\delta}_3)\frac{M_{\text{QCD}}^2}{M_T^2}, \varepsilon\xi\frac{M_{\text{QCD}}^4}{Q^2 M_T^2}, (w, \sigma_{1,8})\frac{M_{NN}^2 M_{\text{QCD}}^2}{Q^2 M_T^2}, \delta_{0,3}\frac{\alpha_{\text{em}}}{4\pi}\frac{M_{\text{QCD}}^2}{M_T^2}\right), \end{aligned} \quad (44)$$

$$\begin{aligned} \text{Fig. 3(a)} &= \mathcal{O}\left(\frac{eG_F}{4\pi M_{\text{QCD}}}\right) \times \\ &\mathcal{O}\left(\bar{\theta}, (\tilde{\delta}_0, \varepsilon\tilde{\delta}_3)\frac{M_{\text{QCD}}^2}{M_T^2}, \varepsilon\xi\frac{M_{\text{QCD}}^4}{Q^2 M_T^2}, (w, \sigma_{1,8})\frac{M_{\text{QCD}}^2}{M_T^2}, \delta_{0,3}\frac{\alpha_{\text{em}}}{4\pi}\frac{M_{\text{QCD}}^2}{M_T^2}\right), \end{aligned} \quad (45)$$

$$\begin{aligned} \text{Fig. 3(b)} &= \mathcal{O}\left(\frac{eG_F Q}{4\pi M_{NN} M_{\text{QCD}}}\right) \times \\ &\mathcal{O}\left(\bar{\theta}, (\tilde{\delta}_0, \varepsilon\tilde{\delta}_3)\frac{M_{\text{QCD}}^2}{M_T^2}, \varepsilon\xi\frac{M_{\text{QCD}}^4}{Q^2 M_T^2}, (w, \sigma_{1,8})\frac{M_{NN}^2 M_{\text{QCD}}^2}{Q^2 M_T^2}, \delta_{0,3}\frac{\alpha_{\text{em}}}{4\pi}\frac{M_{\text{QCD}}^2}{M_T^2}\right), \end{aligned} \quad (46)$$

$$\begin{aligned} \text{Fig. 3(c)} &= \mathcal{O}\left(\frac{eG_F Q}{4\pi M_{\text{QCD}}^2}\right) \times \\ &\mathcal{O}\left(\bar{\theta}, \tilde{\delta}_{0,3}\frac{M_{\text{QCD}}^2}{M_T^2}, \xi\frac{M_{\text{QCD}}^4}{Q^2 M_T^2}, (w, \sigma_{1,8})\frac{M_{\text{QCD}}^4}{Q^2 M_T^2}, (\varepsilon\delta_0\frac{m_\pi^2}{M_{\text{QCD}}}, \delta_3)\frac{M_{\text{QCD}}^2}{M_T^2}\right). \end{aligned} \quad (47)$$

Various statements made in the text about relative magnitudes of the  $P\bar{T}$  sources follow straightforwardly from these relations.

The same NDA technique can be used to estimate the size of other  $P\bar{T}$  contributions. For example, the contributions of short-range  $P\bar{T}$  nucleon-nucleon-photon interactions to the  $P\bar{T}$  form factor of the deuteron are, for all sources, subleading with respect to Figs. 1, 2, and 3. Likewise, short-range  $P\bar{T}$  nucleon-nucleon interactions contribute to the  $P\bar{T}$  two-nucleon



potential at higher order than one-pion exchange diagrams involving  $h_1$  [26]. As a consequence, diagrams involving these interactions are also suppressed compared to the diagrams discussed here. The same holds for diagrams with  $\cancel{P}T$  nucleon-nucleon-photon ( $NNNN\gamma$ ) interactions [22].

In addition, one can understand why effective  $P\cancel{T}$  interactions contribute at higher orders. One-pion exchange with a  $P\cancel{T}$  coupling does not contribute to the  $P\cancel{T}$  potential in the two-nucleon sector [34]. The latter is dominated by exchanges of heavier mesons, like the  $\rho$  and the  $a_1$ , which, at low energy, appear as two-nucleon contact interactions with at least two derivatives (see, *e.g.*, Ref. [39]). The size of these two-nucleon operators can be again estimated in NDA by multiplying the reduced couplings for the  $\cancel{P}T$  and  $P\cancel{T}$  interactions. For example, for the  $\bar{\theta}$  term a  $P\cancel{T}$  two-nucleon coupling would scale as  $\bar{\theta}G_F Q/(4\pi m_N M_{\text{QCD}}^2)$ . Inserting this coupling into a two-loop diagram with the photon interacting on a nucleon line via the nucleon magnetic moment gives rise to a TQM of order  $\mathcal{T}_d = \mathcal{O}(e\bar{\theta}G_F Q^2/((4\pi)^2 M_{\text{QCD}}^3))$ . Such a contribution is much smaller than the long-range component that results from the pion-nucleon couplings  $h_1$  and  $\bar{g}_0$  in Fig. 1, as can be seen from comparison with Eq. (43). Similar power-counting estimates indicate that contributions from diagrams with short-range  $P\cancel{T} NNNN\gamma$  vertices are smaller than the contributions in Eqs. (43)-(47) by at least a factor  $Q^2/M_{\text{NN}}^2$ .

For dimension-six sources, we can neglect  $P\cancel{T}$  operators in the EFT as well. For non-electromagnetic sources such as the qCEDM, the FQLR operators, and the  $\chi$ ISs the argument is analogous to the one used for the  $\bar{\theta}$  term. For the qEDM one might think that  $P\cancel{T}$  pion-nucleon-photon interactions could be relevant. Indeed, a  $P\cancel{T}$  operator of the form  $D_\mu \pi \cdot \bar{N} S^\nu \tau N e F_{\mu\nu}$  gives a nonzero contribution to the deuteron TQM via a two-loop diagram. However, by power counting we find this diagram to be smaller by a factor  $Q^2/M_{\text{QCD}}^2$  compared to the diagram in Fig. 3, which provides the dominant contribution for the qEDM.

## C Form factor integrals

In Sec. 3 the results for the deuteron TQFF  $F_{PT}(\vec{q}^2)$  were expressed in terms of  $L = 1, 2, 3$  loop integrals  $I^{(L)}(\xi, \vec{x})$ , where  $\xi = \gamma/m_\pi$  and  $\vec{x} = \vec{q}/(4\gamma)$ . We list here the form and expansions of these integrals to terms of order  $x^2$ , where  $x = |\vec{x}|$ .

The one-loop integral in Eq. (24) is standard, appearing for example in the deuteron magnetic quadrupole form factor [21]. It has the simple closed form

$$I^{(1)}(\vec{x}) = \frac{\arctan x}{x} . \quad (48)$$

The integrals appearing in the two- and three-loop diagrams are more complicated. We express them in terms of the dimensionless variables  $\vec{y}_i$ , obtained by rescaling the loop momenta,  $\vec{k}_i = m_\pi \vec{y}_i$ . They can be conveniently calculated in coordinate space [40, 18].

The two-loop functions in Eqs. (21), (24), and (25) depend on three two-loop integrals,

$$I_1^{(2)}(\xi, \vec{x}) = \frac{1}{x^2(2\pi)^4} \int d^3y_1 d^3y_2 \frac{\vec{y}_2 \cdot \vec{x}}{\vec{y}_2^2 + 1} \frac{1}{\vec{y}_1^2 + \xi^2} \frac{1}{(\vec{y}_1 + \vec{y}_2)^2 + \xi^2} \frac{1}{(\vec{y}_1 + 2\xi\vec{x})^2 + \xi^2}, \quad (49)$$

$$I_2^{(2)}(\xi, \vec{x}) = \frac{1}{x^4(2\pi)^4} \int d^3y_1 d^3y_2 \left( \vec{y}_2 \cdot \vec{x} \vec{y}_1 \cdot \vec{x} - \frac{x^2}{3} \vec{y}_1 \cdot \vec{y}_2 \right) \frac{1}{\vec{y}_1^2 + \xi^2} \frac{1}{(\vec{y}_1 + \vec{y}_2)^2 + \xi^2} \frac{1}{\vec{y}_2^2 + 1} \frac{1}{(\vec{y}_1 + 2\xi\vec{x})^2 + \xi^2}, \quad (50)$$

$$I_3^{(2)}(\xi, \vec{x}) = \frac{1}{x^4(2\pi)^4} \int d^3y_1 d^3y_2 \left( \vec{y}_2 \cdot \vec{x} \vec{y}_1 \cdot \vec{x} - \frac{x^2}{3} \vec{y}_1 \cdot \vec{y}_2 \right) \frac{1}{\vec{y}_1^2 + \xi^2} \frac{1}{(\vec{y}_1 + \vec{y}_2)^2 + \xi^2} \frac{1}{(\vec{y}_2 + 2\xi\vec{x})^2 + 1} \frac{1}{(\vec{y}_2 - 2\xi\vec{x})^2 + 1}. \quad (51)$$

Expanding in  $\vec{x}^2$  and retaining the first two terms in the expansion, we find

$$I_1^{(2)}(\xi, \vec{x}) = \frac{1 + \xi}{12(1 + 2\xi)^2} - x^2 \frac{10 + 65\xi + 144\xi^2 + 72\xi^3}{360(1 + 2\xi)^4} + \mathcal{O}(x^4), \quad (52)$$

$$I_2^{(2)}(\xi, \vec{x}) = -\frac{10 + 27\xi + 18\xi^2}{540(1 + 2\xi)^3} + x^2 \frac{70 + 595\xi + 1918\xi^2 + 2400\xi^3 + 960\xi^4}{12600(1 + 2\xi)^5} + \mathcal{O}(x^4), \quad (53)$$

$$I_3^{(2)}(\xi, \vec{x}) = -\frac{\xi(4 + 21\xi + 30\xi^2)}{540(1 + 2\xi)^3} + x^2 \frac{\xi^3(68 + 590\xi + 1820\xi^2 + 2100\xi^3 + 840\xi^4)}{4725(1 + 2\xi)^5} + \mathcal{O}(x^4). \quad (54)$$

The two-loop functions  $I_{a,b,c,d}^{(2)}$  are obtained from  $I_{1,2,3}^{(2)}$  by multiplying them by prefactors that take into account spin and isospin factors, and the symmetry factor of each diagram:

$$I_a^{(2)}(\xi, \vec{x}) = 12I_2^{(2)}(\xi, \vec{x}) + 4I_1^{(2)}(\xi, \vec{x}), \quad (55)$$

$$I_b^{(2)}(\xi, \vec{x}) = 24I_3^{(2)}(\xi, \vec{x}), \quad (56)$$

$$I_c^{(2)}(\xi, \vec{x}) = 48I_1^{(1)}(\xi, \vec{x}), \quad (57)$$

$$I_d^{(2)}(\xi, \vec{x}) = -48I_2^{(2)}(\xi, \vec{x}) - 8I_1^{(2)}(\xi, \vec{x}). \quad (58)$$

Similarly, the three-loop functions that enter in Eq. (20) are defined in terms of two three-loop tensor integrals,

$$I_1^{(3)}(\xi, \vec{x}) = \frac{1}{2\xi x^4(2\pi)^6} \int d^3y_1 d^3y_2 d^3y_3 \left( \vec{y}_2 \cdot \vec{x} \vec{y}_3 \cdot \vec{x} - \frac{x^2}{3} \vec{y}_2 \cdot \vec{y}_3 \right) \frac{1}{\vec{y}_1^2 + \xi^2} \frac{1}{\vec{y}_3^2 + 1} \frac{1}{(\vec{y}_1 + \vec{y}_3)^2 + \xi^2} \frac{1}{\vec{y}_2^2 + 1} \frac{1}{(\vec{y}_1 + 2\xi\vec{x})^2 + \xi^2} \frac{1}{(\vec{y}_1 + \vec{y}_2 + 2\xi\vec{x})^2 + \xi^2}, \quad (59)$$

$$I_2^{(3)}(\xi, \vec{x}) = \frac{1}{2\xi x^4(2\pi)^6} \int d^3y_1 d^3y_2 d^3y_3 \left( \vec{y}_2 \cdot \vec{x} \vec{y}_3 \cdot \vec{x} - \frac{x^2}{3} \vec{y}_2 \cdot \vec{y}_3 \right) \frac{1}{\vec{y}_1^2 + \xi^2} \frac{1}{\vec{y}_3^2 + 1} \frac{1}{(\vec{y}_1 + \vec{y}_3)^2 + \xi^2} \frac{1}{(\vec{y}_2 + 2\xi\vec{x})^2 + 1} \frac{1}{(\vec{y}_2 - 2\xi\vec{x})^2 + 1} \frac{1}{(\vec{y}_1 + \vec{y}_2)^2 + \xi^2}, \quad (60)$$

which are finite in three and four dimensions. Again retaining terms up to order  $\mathcal{O}(x^2)$ ,

$$\begin{aligned}
I_1^{(3)}(\xi, \vec{x}) = & \frac{15 + 75\xi + 110\xi^2 + 30\xi^3 - 12\xi^4 + 8\xi^5 - 48\xi^6}{2160\xi^5(1+2\xi)^3} \log\left(\frac{2(1+\xi)}{1+2\xi}\right) \\
& + \frac{15 + 65\xi + 75\xi^2 + 7\xi^3 - 30\xi^4 - 12\xi^5 - 24\xi^6}{4320\xi^4(1+\xi)(1+2\xi)^3} - \frac{1}{288\xi^6} \left( \text{Li}_2\left(-\frac{1}{1+2\xi}\right) + \frac{\pi^2}{12} \right) \\
& - x^2 \left[ \frac{1}{37800\xi^5(1+2\xi)^5} (105 + 945\xi + 3290\xi^2 + 5390\xi^3 + 3836\xi^4 + 560\xi^5 \right. \\
& \left. - 160\xi^6 + 80\xi^7 - 4320\xi^8 - 9024\xi^9 - 5760\xi^{10}) \log\left(\frac{2(1+\xi)}{1+2\xi}\right) \right. \\
& \left. + \frac{1}{75600\xi^4(1+\xi)^3(1+2\xi)^5} (105 + 1085\xi + 4260\xi^2 + 10374\xi^3 + 12789\xi^4 \right. \\
& \left. + 6765\xi^5 - 5202\xi^6 - 10052\xi^7 + 5400\xi^8 + 24384\xi^9 + 20544\xi^{10} + 5760\xi^{11}) \right. \\
& \left. - \frac{1}{720\xi^6} \left( \text{Li}_2\left(-\frac{1}{1+2\xi}\right) + \frac{\pi^2}{12} \right) \right] + \mathcal{O}(x^4)
\end{aligned} \tag{61}$$

and

$$\begin{aligned}
I_2^{(3)}(\xi, \vec{x}) = & \frac{\xi}{540(1+2\xi)^3} \left[ \frac{7 + 44\xi + 58\xi^2 + 20\xi^3}{4(1+\xi)^2} - (1+6\xi) \log\left(\frac{2(1+\xi)}{1+2\xi}\right) \right] \\
& + x^2 \frac{\xi^3}{90(1+2\xi)^5} \left[ \frac{5 + 50\xi + 116\xi^2 + 72\xi^3}{3} \log\left(\frac{2(1+\xi)}{1+2\xi}\right) \right. \\
& \left. + \frac{205 + 2494\xi + 12290\xi^2 + 29472\xi^3 + 37540\xi^4 + 25672\xi^5 + 8720\xi^6 + 1120\xi^7}{280(1+\xi)^4} \right] \\
& + \mathcal{O}(x^4),
\end{aligned} \tag{62}$$

where  $\text{Li}_2(x)$  is the dilogarithm function. The function  $I_2^{(3)}$  vanishes in the limit of vanishing binding momentum,  $\xi \rightarrow 0$ .  $I_1^{(3)}(\xi, 0)$  consists of the sum of three terms, each of them divergent for  $\xi \rightarrow 0$ . Because of cancellations between these terms,  $I_1^{(3)}(\xi, 0)$  has a finite limit for vanishing  $\xi$ ,  $I_1^{(3)}(0, 0) = -1/162$ . However, this limit is not a good approximation to the value of the three-loop function at the physical value of  $\xi$ ,  $\xi \simeq 0.3$ . One needs to keep at least terms up to  $\xi^{15}$  to obtain an approximation of  $I_1^{(3)}(0.3, 0)$  at the 10% accuracy.

As before, lumping spin, isospin, and symmetry factors in the definitions of  $I_{a,b}^{(3)}$ , we have

$$I_a^{(3)}(\xi, \vec{x}) = 36 I_1^{(3)}(\xi, \vec{x}), \quad I_b^{(3)}(\xi, \vec{x}) = 240 I_2^{(3)}(\xi, \vec{x}). \tag{63}$$

## References

- [1] I.B. Khriplovich and S.K. Lamoreaux, *CP Violation Without Strangeness: Electric Dipole Moments of Particles, Atoms, and Molecules* (Springer Verlag, Berlin, 1997).
- [2] Ya.B. Zel'dovich, Sov. Phys. JETP **6** (1958) 1184; **12** (1961) 777.
- [3] V. Glaser and B. Jakšić, Nuovo Cim. **5** (1957) 76; I.Yu. Kobzarev, L.B. Okun', and M.V. Terent'ev, JETP Lett. **2** (1965) 289; A.D. Dolgov, JETP Lett. **2** (1965) 308.

- [4] C.G. Gray, G. Karl, and V.A. Novikov, Am. J. Phys. **78** (2010) 936.
- [5] F. Boudjema and C. Hamzaoui, Phys. Rev. D **43** (1991) 3748.
- [6] S.G. Porsev, Phys. Rev. A **49** (1994) 5105.
- [7] V.M. Dubovik and A.A. Cheshkov, Sov. Phys. JETP **24** (1967) 111; V.M. Dubovik, E.P. Likhtman, and A.A. Cheshkov, Sov. Phys. JETP **25** (1967) 464; D. Schildknecht, Z. Phys. **201** (1967) 99; R. Prepost, R.M. Simonds, and B.H. Wiik, Phys. Rev. Lett. **21** (1968) 1271; K.Y. Lin, Nucl. Phys. B **18** (1970) 162; H. Arenhövel and S.K. Singh, Eur. Phys. J. A **10** (2001) 183.
- [8] P.D. Eversheim, B. Lorentz, and Yu. Valdau (spokespersons), Test of Time-Reversal Invariance in Proton-Deuteron Scattering at COSY, [http://apps.fz-juelich.de/pax/paxwiki/index.php/Test\\_of\\_Time-Reversal\\_Invariance\\_at\\_COSY\\_\(TRIC\)](http://apps.fz-juelich.de/pax/paxwiki/index.php/Test_of_Time-Reversal_Invariance_at_COSY_(TRIC)); P.D. Eversheim *et al.*, Hyperfine Interact. **193** (2009) 335; Yu. Valdau, POS **STOR11** 013; M. Beyer, Nucl. Phys. A **560** (1993) 895.
- [9] C. Jarlskog, Phys. Rev. Lett. **55** (1985) 1039.
- [10] G. 't Hooft, Phys. Rev. Lett. **37** (1976) 8; Phys. Rev. D **14** (1976) 3432, *ibid.* **18** (1978) 2199(E).
- [11] C.A. Baker *et al.*, Phys. Rev. Lett. **97** (2006) 131801.
- [12] J. Engel, P.H. Frampton, and R.P. Springer, Phys. Rev. D **53** (1996) 5112; M.J. Ramsey-Musolf, Phys. Rev. Lett. **83** (1999) 3997, *ibid.* **84** (2000) 5681(E); A. Kurylov, G.C. McLaughlin, and M.J. Ramsey-Musolf, Phys. Rev. D **63** (2001) 076007.
- [13] P.F. Bedaque and U. van Kolck, Ann. Rev. Nucl. Part. Sci. **52** (2002) 339.
- [14] V. Bernard, N. Kaiser, and U.-G. Meißner, Int. J. Mod. Phys. E **4** (1995) 653.
- [15] C.M. Maekawa and U. van Kolck, Phys. Lett. B **478** (2000) 73; C.M. Maekawa, J.S. Veiga, and U. van Kolck, Phys. Lett. B **488** (2000) 167.
- [16] W.H. Hockings and U. van Kolck, Phys. Lett. B **605** (2005) 273; K. Ottnad, B. Kubis, U.-G. Meißner, and F.-K. Guo, Phys. Lett. B **687** (2010) 42; J. de Vries, E. Mereghetti, R.G.E. Timmermans, and U. van Kolck, Phys. Lett. B **695** (2011) 268; E. Mereghetti, J. de Vries, W.H. Hockings, C.M. Maekawa, and U. van Kolck, Phys. Lett. B **696** (2011) 97.
- [17] D.B. Kaplan, M.J. Savage, and M.B. Wise, Nucl. Phys. B **534** (1998) 329.
- [18] S. Fleming, T. Mehen, and I.W. Stewart, Nucl. Phys. A **677** (2000) 313.
- [19] S.R. Beane, P.F. Bedaque, M.J. Savage, and U. van Kolck, Nucl. Phys. A **700** (2002) 377; A. Nogga, R.G.E. Timmermans, and U. van Kolck, Phys. Rev. C **72** (2005) 054006; M. Birse, Phys. Rev. C **74** (2006) 014003; M. Pavón Valderrama, Phys. Rev. C **83** (2011) 024003; **84** (2011) 064002; B. Long and C.J. Yang, Phys. Rev. C **84** (2011) 057001; **85** (2012) 034002; **86** (2012) 024001.
- [20] D.B. Kaplan, M.J. Savage, and M.B. Wise, Phys. Rev. C **59** (1999) 617.

- [21] J. de Vries, E. Mereghetti, R.G.E. Timmermans, and U. van Kolck, Phys. Rev. Lett. **107** (2011) 091804.
- [22] M.J. Savage and R.P. Springer, Nucl. Phys. A **686** (2001) 41.
- [23] S. Weinberg, *The Quantum Theory of Fields*, Vol. 2 (Cambridge University Press, Cambridge, 1996).
- [24] A.V. Manohar and H. Georgi, Nucl. Phys. B **234** (1984) 189; H. Georgi and L. Randall, Nucl. Phys. B **276** (1986) 241.
- [25] D.B. Kaplan and M.J. Savage, Nucl. Phys. A **556** (1993) 653; *ibid.* **570** (1994) 833(E); **580** (1994) 679(E).
- [26] S.L. Zhu, C.M. Maekawa, B.R. Holstein, M.J. Ramsey-Musolf, and U. van Kolck, Nucl. Phys. A **748** (2005) 435.
- [27] D.B. Kaplan, M.J. Savage, and R.P. Springer, Phys. Lett. B **449** (1999) 1.
- [28] M.T. Gericke *et al.*, Phys. Rev. C **83** (2011) 015505.
- [29] J. Wasem, Phys. Rev. C **85** (2012) 022501.
- [30] W. Buchmüller and D. Wyler, Nucl. Phys. B **268** (1986) 621; B. Grzadkowski, M. Iskrzynski, M. Misiak, and J. Rosiek, JHEP **1010** (2010) 085.
- [31] J. de Vries, E. Mereghetti, R.G.E. Timmermans, and U. van Kolck, Ann. Phys. (to appear), [arXiv:1212.0990 \[hep-ph\]](#).
- [32] E. Mereghetti, W.H. Hockings, and U. van Kolck, Ann. Phys. **325** (2010) 2363.
- [33] R.J. Crewther, P. Di Vecchia, G. Veneziano, and E. Witten, Phys. Lett. B **88** (1979) 123; **91** (1980) 487(E).
- [34] M. Simonius, Phys. Lett. B **58** (1975) 147.
- [35] J. de Vries, R. Higa, C.-P. Liu, E. Mereghetti, I. Stetcu, R.G.E. Timmermans, and U. van Kolck, Phys. Rev. C **84** (2011) 065501; C.-P. Liu, J. de Vries, E. Mereghetti, R.G.E. Timmermans, and U. van Kolck, Phys. Lett. B **713** (2012) 447.
- [36] W. Dekens and J. de Vries, JHEP (to appear), [arXiv:1303.3156 \[hep-ph\]](#).
- [37] S.R. Beane, K. Orginos, and M.J. Savage, Nucl. Phys. B **768** (2007) 38.
- [38] J. de Vries, Ph.D. dissertation, University of Groningen (2012).
- [39] Y.H. Song, R. Lazauskas, and V. Gudkov, Phys. Rev. C **83** (2011) 065503.
- [40] M. Binger, [nucl-th/9901012](#).